

Silicon interaction with low-electronegativity metals: Interdiffusion and reaction at the Ca/Si(111) interface

A. Franciosi and J. H. Weaver

Department of Chemical Engineering and Materials Science, University of Minnesota, Minneapolis, Minnesota 55455

D. T. Peterson

Ames Laboratory, U. S. Department of Energy and Department of Materials Science, Iowa State University, Ames, Iowa 50011

(Received 26 November 1984)

We present the first photoemission study of reactions which occur at an alkali-earth-silicon interface. Room-temperature results indicate extensive atomic interdiffusion with substantial ionic bonding. Analysis of the Si 2*p* core line shape, the Ca 3*p* core levels, the many-body losses, and the valence bands shows that the first reaction product ($1 \leq \Theta \leq 12 \text{ \AA}$) corresponds to a weakly metallic Ca-Si phase. A second component is Ca-rich but has Si present in two different bonding configurations. Core line-shape analysis facilitates evaluation of interface atomic concentrations and discussions of morphology.

Studies of metal-silicon junction formation using surface-sensitive spectroscopic techniques have been able to provide a microscopic picture of interface interactions and morphologies.¹ It has recently been established, for example, that simple metals on silicon exhibit relatively sharp interfaces² and the noble and transition metals react with Si at room temperature to produce diffuse interfaces with silicidlike phases of variable depth (Ag and V are notable exceptions^{3,4}). In general, Schottky barrier formation for these metal-Si junctions induces relatively little change in band bending [0.1–0.2 eV as compared to the clear Si(111)-2×1 surface⁵].

Despite the enormous amount of work represented by Refs. 1–5 (and the 1050 references cited by Brillson¹), little attention has been devoted to rare-earth or alkali-earth metal overlayers on Si. Because of the low *d*-electron count of these metals, their interfaces should be intriguingly different from those involving transition metals. In particular, the low *d*-electron count and low electronegativity of the metals should alter the picture of interface chemistry dominated by strong metal-*d*-silicon-*p* covalent bonds and minimal charge transfer.^{6–8} Likewise, these interfaces should differ from simple-metal-silicon junctions because of large electronegativity differences. As far as interface parameters are concerned, qualitative differences in evolution are suggested by the low Schottky barrier heights of several rare-earth-disilicide-silicon junctions,⁹ i.e., 0.3–0.4 eV lower than those reported for simple, transition, and noble metals on silicon.

In this paper we discuss synchrotron radiation photoemission investigations of Ca/Si(111) interface formation. These are the first such alkali-earth-silicon studies, and they build on previous work with Sm/Ge(111) and Sm/Si(111),¹⁰ high-resolution investigations of Ce reactions on Si(111), Ge(111), and GaAs(110),¹¹ and results for Yb/Si.¹² Our results show a reacted region with Ca-Si intermixing followed by one in which a Ca-rich overlayer

evolves at room temperature. Each region has characteristic valence-band emission, Ca 3*p* line shape, and Si 2*p* core binding energies. In the first stage, ionicity plays a major role in determining the electronic structure but, surprisingly, we find no change in band bending, i.e., the ionic contribution to the chemical bonds of the extended interface region does not affect the equilibrium barrier value to within 0.1 eV. The second stage, $\Theta \geq 12 \text{ \AA}$, has metallic character corresponding to evolving Ca-derived valence bands, but Si continues to be present in small quantities in two inequivalent chemical states.

The experiments were performed at the Synchrotron Radiation Center. Clean Si(111)-2×1 surfaces (*n*-type silicon, P-doped, $n \sim 10^{15} \text{ cm}^{-3}$) were produced by cleavage in the photoelectron spectrometer (operating pressure $\sim 5 \times 10^{-11}$ Torr). Monochromatic radiation was obtained from a 3-m toroidal grating monochromator, and photoelectrons were energy analyzed by a double-pass cylindrical mirror analyzer. The overall experimental resolution was 0.4–0.5 eV for the valence band and Ca 3*p* results and ~ 1 eV for the Si 2*p* core studies at $h\nu = 135$ eV.

The interfaces were prepared by direct sublimation of ultrahigh purity, vacuum distilled Ca from a W coil. The overlayer thickness, Θ , was measured by a quartz crystal monitor and is given in angstrom units [1 monolayer = 1ML = 3.35 Å using the Si(111) surface atomic density of $7.8 \times 10^{14} \text{ cm}^{-2}$]. During evaporation, the pressure rose as hydrogen was released from the Ca source itself ($\leq 6 \times 10^{-10}$ Torr). Subsequent controlled exposure to much higher pressures of hydrogen produced minimal effects, and we conclude that the results presented here are representative of pristine Ca-Si interactions. Studies of the interface were carried out for metal coverages of 0.25 to 100 Å on room temperature Si substrates. Radiant heating from the evaporator was negligible because of the geometry of the system and the very low power needed to

evaporate Ca.

Valence-band studies were performed at photon energies of 40 and 60 eV, as well as 12 eV to emphasize the Si bulk valence-band features and monitor variations in band bending at low Ca coverage. In Fig. 1 we show photoelectron energy distribution curves (EDC's) for the valence bands of Ca/Si(111) taken at $h\nu=60$ eV. The bottommost EDC represents clean Si(111) and spectra displaced upward show the effect of Ca intermixing. The topmost EDC was obtained from a 450 Å Ca film evaporated onto oxidized copper and is representative of Ca metal. The valence-band results at 40 eV photon energy are virtually identical to those shown in Fig. 1 and are not shown here.

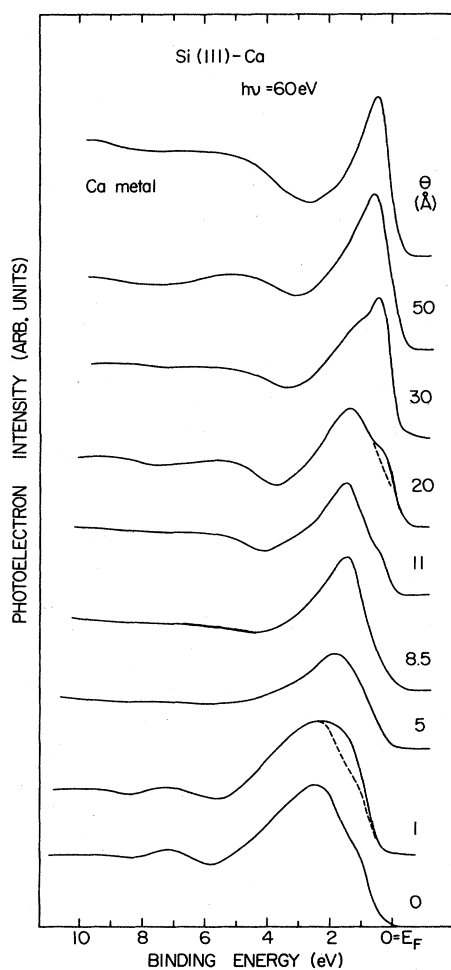


FIG. 1. Valence-band photoelectron energy distribution curves (EDC's) for the Ca/Si(111) interface at room temperature. The bottommost spectrum corresponds to the clean Si(111)- 2×1 surface, the topmost EDC to a 450 Å Ca film evaporated on an inert substrate. Broad emission features at 4.9 and 9.6 eV correspond to plasmon losses. The first interface reaction state ($0 < \Theta < 12$ Å) yields a weakly metallic Ca-Si intermixed phase with substantial ionic bonding character. At higher metal coverages Ca-rich phases dominate the interface valence emission.

The valence bands of calcium metal (Fig. 1) are dominated by emission within 2 eV of E_F with a full width at half maximum (FWHM) ~ 1.1 eV. Broad emission features at 4.9 and ~ 9.6 eV (4.5 and 9.1 eV below the valence-band peak) have been interpreted¹³⁻¹⁶ as plasmons excited during the photoemission process. In contrast, EDC's for Ca coverage $1 \leq \Theta \leq 12$ Å show valence-band emission centered ~ 1.4 eV below E_F which increases with Θ while the Si valence-band features at -7.5 and -10.5 eV, typical of sp^3 hybridization, attenuate rapidly. Indeed, by $\Theta=5$ Å=1.5 ML, these Si substrate features are gone. For $\Theta \approx 10$ Å, the spectra are relatively stable, exhibiting broad emission 1.4 eV below E_F (FWHM 1.9–2 eV), very low emission at E_F , and no plasmons (see Fig. 1, $\Theta=8.5$ Å). Increasing the coverage above ~ 10 Å results in new structure 0.3–0.4 eV below E_F , as seen by the weak shoulder for 11 Å. This shoulder is pronounced for ~ 20 Å and its growth is accompanied by the emergence of broad plasmon loss features at 4.9 and 9.6 eV. By $\Theta \approx 30$ Å, the emission near E_F is almost Ca-like, but complete convergence to Ca requires ~ 100 Å coverage.

These valence-band results indicate that during the first reaction stage a large number of states form ~ 1.4 eV below E_F . Given the large chemical shifts observed and the electronegativity differences (next paragraphs), these can be identified as largely Si p derived. The very low density of states near E_F indicates that the Ca d states are nearly empty in the interface-stabilized silicide and p - d mixing is not strong. Hence, we conclude that ionic bonds are important in the Ca/Si interface reaction. With increasing coverage, states near E_F become visible and ultimately dominate. Their emergence indicates the gradual covering up of the reacted layer by a Ca-rich film having partially occupied $3d$ states and metallic bonding.¹³

In Fig. 2 we show Ca $3p$ core EDC's for $h\nu=60$ eV displaced with arbitrary units to emphasize line-shape changes. As discussed elsewhere,¹³⁻¹⁶ the complex Ca $3p$ line shape is due to final-state effects which, for our purposes here, can be used to fingerprint the evolution of the interface electronic structure. The results for $\Theta=1$ Å show a single unresolved $3p$ emission feature 25.4 eV below E_F and no high-energy losses. With coverage, the core broadens, shifts to lower binding energy, and extensive, featureless emission increases on the high-energy side of the core. At $\Theta=15$ Å, structure ~ 1.6 eV deeper than the main line becomes distinguishable and a satellite is evident near 29 eV. The appearance of these defines the onset of multielectron effects¹³ where d screening and multiplet final states are possible. Thus, both core studies and valence-band studies indicate that the overlayer becomes increasingly calcium-rich with increased emission at E_F , better d screening of the photohole, and greater probability of plasmon excitation.

In Fig. 3 we show selected Si $2p$ core EDC's for $h\nu=135$ eV (solid line). The zero of the binding-energy scale corresponds to the initial position of the Si $2p$ level for Si(111)- 2×1 . Again, the EDC's have been scaled to emphasize the line-shape changes. The bottommost spectrum for clean Si(111) shows an unresolved spin-orbit splitting and FWHM of 1.65 eV. These results show sig-

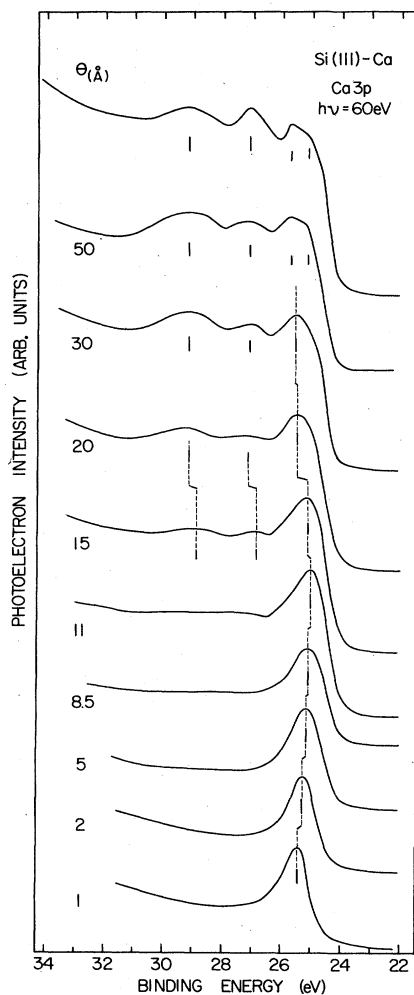


FIG. 2. EDC's for the Ca 3*p* core emission from the Ca/Si(111) interface. The topmost spectrum corresponds to the bulk Ca 3*p* core emission. The complex Ca 3*p* line shape is due to multielectron final-state effects associated with metallic *d* screening. That screening channel is not observed during the first interface formation stage when mostly ionic reaction products are formed.

nificant variations in binding energies and overall FWHM as the environment of the Si within the photoelectron escape depth changes. At $\Theta = 1$ Å, the distorted line shape indicates that reaction has already begun. At $\Theta = 5$ Å, the reacted line is clearly visible 1.1 eV from the main line. At $\Theta = 15$ Å, the reacted line dominates and is comparable in width to the unreacted component for the clean surface. At $\Theta = 30$ Å the core emission is again wider, indicating the presence of two or more Si environments near the surface.

Quantitative line-shape deconvolutions of the 2*p* line reveal the coverage dependence of each Si species present in the interface. Gaussian line shapes with 1.65 eV FWHM were used since the measured spectral width was determined primarily by the overall experimental resolution at 135 eV. The binding energies and intensities were

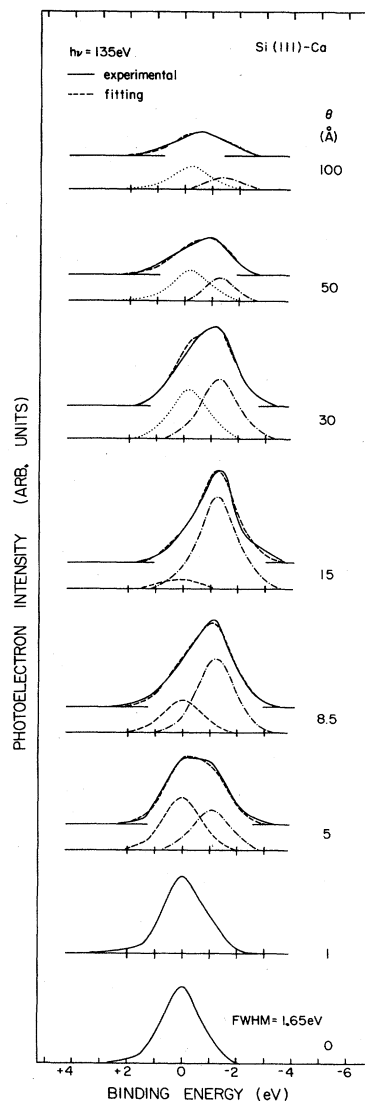


FIG. 3. EDC's for the Si 2*p* core emission from the Ca/Si(111) interface (solid line). Superimposed to the experimental spectra we show (dashed line) the result of a fit in terms of a Si 2*p* "substrate" component (dashed line), a "phase-1" Si 2*p*-reacted component (dot-dashed line), and a "phase-2" Si 2*p*-reacted component. The phase-1 component corresponds to a Ca-Si intermixed configuration with mostly ionic bonding character. The phase-2 component corresponds to Si with lower Ca coordination, probably at the surface.

used as fitting parameters. In light of these simplifications, the results shown in Fig. 3 are remarkably good. For $1 < \Theta < 15$ Å the fitting required a substrate contribution at fixed binding energy (dashed line) and a stage-1 reacted component shifted 1.1–1.35 eV (dot-dashed line). Spectra at coverages above 15 Å were fitted with a stage-1 component and a final Si 2*p* line which emerged 0.3 eV below the initial Si 2*p* position (dotted line).

In the upper part of Fig. 4 we show the overall attenuation of the Si 2*p* emission, defined as $\ln I(\Theta)/I(0)$, where

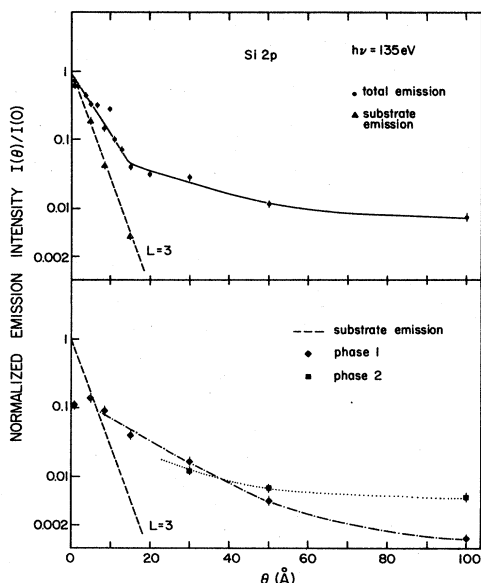


FIG. 4. Top: Attenuation of the overall Si 2*p* integrated emission normalized to the initial Si 2*p* emission. Bottom: Attenuation for each of the Si 2*p* components identified from the fitting procedure in Fig. 3. Attenuation of the unreacted substrate component (dashed line) is much faster than is reasonable for an escape-depth-driven mechanism and reflects intermixing at the interface with conversion of substrate atoms into reacted stage-1 Si. The slow attenuation of the two Si 2*p*—reacted components indicate that Si out-diffuses into the Ca layer but that the amount present near the surface diminishes as the overlayer becomes thicker.

$I(\Theta)$ is the integrated emission normalized to the photon flux at a coverage Θ and $I(0)$ is the emission for the clean surface. In the lower panel, we show the attenuation of the three components of Fig. 3. Results for the overall Si 2*p* core emission (top) show exponential attenuation for $1 < \Theta < 15$ Å, a sharp change in slope at $\Theta \sim 15$ Å, and much slower attenuation at high coverage. Analysis of the unreacted substrate component (dashed line) shows exponential attenuation consistent with an escape-depth-driven behavior but with a slope that is much steeper than is reasonable for photoelectrons with ~ 30 eV kinetic energy (apparent escape depth ≤ 3 Å instead of 5–7 Å). This behavior is consistent with intermixing at the interface with conversion of substrate Si atoms into reacted stage-1 Si.

The attenuation of the two reacted components (dot-dashed and dotted lines) is much slower than expected for an escape-depth-driven mechanism involving formation of a continuous Ca film over the reacted interface, as might have been suggested by high-coverage valence-band studies alone. Instead, the results of Fig. 4 indicate that Si out-diffuses into the Ca layer, but that the amount present

near the surface diminishes as the overlayer becomes thicker (increasingly Ca-rich). Nevertheless, the binding-energy studies indicate that the local bonding of Si is similar to that in the fully reacted region, again consistent with the very large electronegativity differences and the tendency of Ca and Si in the bulk to form local ionic bonds. At the same time, the second shifted Si component which appears after the metal overlayer has begun to form (15–20 Å) has an intermediate binding energy indicative of reduced bonding with Ca (less charge transfer). With increasing coverage, this second Si component becomes dominant, although it should be noted that it amounts to only 0.6% of the original Si signal at 100 Å. Its small concentration, reduced binding energy persistence at high coverage, and simultaneous presence with the first reacted species suggests that it be identified as surface-diffused Si on the Ca overlayer. Such species have been previously identified for other systems, including Ce/Si(111) (Ref. 11) where it was possible to correlate the onset of surface Si with the early formation of a metal overlayer.

The Si 2*p* line-shape fitting of Fig. 3 was quite sensitive to the energy and should be able to detect changes in binding energy of the substrate Si 2*p* of ≤ 0.1 eV. Since no changes were observed, we conclude that the complex formation chemistry does not change the barrier height within experimental uncertainty (0.1 eV). This invariance is consistent with valence-band results at $h\nu = 12$ eV that show no change of the bulk Si valence-band features at low metal coverages and indicate no change in band bending. The resulting 0.75 eV Schottky barrier is in agreement with the values reported for most transition-metal–Si interfaces⁵ and Sm/Si(111) (Ref. 10) at room temperature, and in contrast with values reported from transport measurements of some rare-earth-disilicide–Si interfaces⁹ and photoemission studies of Ce–Si.¹¹

It is intriguing that the Ca–Si and Ce–Si interfaces show very different behavior at low coverage. In an earlier paper,¹¹ we showed that Ce on Si interacts weakly and forms clusters. Here we report that Ca induces spontaneous reaction by $\Theta = 1$ Å (0.3 ML). Further, Ce on Si results in band-bending changes of 200 meV while Ca does not. Finally, the Ce–Si interface is highly heterogeneous as a consequence of the initial formation of clusters while Ca–Si appears more homogeneous across the surface. Both systems, however, show Si out-diffusion to the surface and have three different Si features which can be readily resolved and followed as a function of coverage to identify the morphology of the extended interface.

It is a pleasure to thank Dr. M. Grioni, Professor L. Braicovich, and Professor A. Fujimori for interesting discussions. This work was supported by the U.S. Army Research Office under Grant No. ARO-DAAG29-83-K-0061. The Synchrotron Radiation Center is supported by the National Science Foundation, and the assistance of its staff is gratefully acknowledged.

¹L. J. Brillson, *Surf. Sci. Rep.* 2, 123 (1982).

²G. Margaritondo, S. B. Christman, and J. E. Rowe, *J. Vac. Sci.*

Technol. 13, 329 (1976); G. Margaritondo, J. E. Rowe, and S. B. Christman, *Phys. Rev. B* 14, 5396 (1976).

- ³While there is still some controversy about the character of the Si/Ag interface, most authors agree that the room-temperature interface exhibits very little, if any, atomic interdiffusion. See, M. Housley, R. Heckingbottom, and C. J. Todd, *Surf. Sci.* **68**, 179 (1977); M. Saitoh, F. Shoji, K. Oura, and T. Hanawa, *ibid.* **112**, 306 (1981); G. Rossi, I. Abbati, L. Braicovich, I. Lindau, and W. E. Spicer, *ibid.* **112**, L765 (1981); J. Stöhr and R. Jaeger, *J. Vac. Sci. Technol.* **21**, 619 (1982); A. L. Wachs, T. Miller, and T.-C. Chiang, *Phys. Rev. B* **29**, 2286 (1984).
- ⁴J. G. Clabes, G. W. Rubloff, and T. Y. Tan, *Phys. Rev. B* **29**, 1540 (1984).
- ⁵P. S. Ho, *J. Vac. Sci. Technol. A* **1**, 745 (1983); R. Purtell, G. Hollinger, G. W. Rubloff, and P. S. Ho, *ibid.* **1**, 566 (1983).
- ⁶O. Bisi and C. Calandra, *J. Phys. C* **14**, 5479 (1981); O. Bisi and L. W. Chiao, *Phys. Rev. B* **25**, 4943 (1982).
- ⁷A. Franciosi and J. H. Weaver, *Surf. Sci.* **132**, 324 (1983).
- ⁸J. H. Weaver, A. Franciosi, and V. L. Moruzzi, *Phys. Rev. B* **29**, 3293 (1984).
- ⁹S. S. Lau, C. S. Pai, C. S. Wu, T. F. Kuech, and B. X. Liu, *Appl. Phys. Lett.* **41**, 77 (1982); K. N. Tu, R. D. Thompson, and B. Y. Tsaur, *ibid.* **38**, 626 (1981).
- ¹⁰A. Franciosi, J. H. Weaver, P. Perfetti, A. D. Katnani, and G. Margaritondo, *Solid State Commun.* **47**, 427 (1983); A. Franciosi, P. Perfetti, A. D. Katnani, J. H. Weaver, and G. Margaritondo, *Phys. Rev. B* **29**, 5611 (1984).
- ¹¹M. Grioni, J. Joyce, S. A. Chambers, D. G. O'Neill, M. del Giudice, and J. H. Weaver, *Phys. Rev. B* **30**, 7370 (1984); *Phys. Rev. Lett.* **53**, 2331 (1984).
- ¹²G. Rossi, J. Nogami, I. Lindau, L. Braicovich, I. Abbati, U. del Pennino, and S. Nannarone, *J. Vac. Sci. Technol. A* **1**, 781 (1983).
- ¹³A. Fujimori, J. H. Weaver, and A. Franciosi, *Phys. Rev. B* **31**, 3549 (1985).
- ¹⁴L. Ley, G. P. Kerker, and N. Mårtensson, *Phys. Rev. B* **23**, 2710 (1981).
- ¹⁵L. Ley, N. Mårtensson, and J. Azouly, *Phys. Rev. Lett.* **45**, 1516 (1980).
- ¹⁶D. R. Penn, *Phys. Rev. Lett.* **38**, 1429 (1977).